Case Studies in Construction Materials 17 (2022) e01451

Contents lists available at ScienceDirect

Case Studies in Construction Materials

journal homepage: www.elsevier.com/locate/cscm

Case study

Long-term performance assessment of a warm recycled motorway pavement

Sara Spadoni [*,1], Lorenzo Paolo Ingrassia [2], Eugenio Mariani, Fabrizio Cardone [3], Francesco Canestrari [4]

Università Politecnica delle Marche, Via Brecce Bianche, 60131 Ancona, Italy

ARTICLE INFO

Keywords:
Warm mix asphalt (WMA)
Field trial
Long-term performance
Fatigue
Viscoelastic continuum damage (VECD)

ABSTRACT

In the last decade, warm mix asphalt (WMA) technologies have undergone a strong development in the pavement sector. In fact, the reduction of the production and compaction temperatures up to 40 °C with respect to the conventional hot mix asphalt (HMA) mixtures has many environmental beneficial effects. However, the long-term field performance of WMA mixtures is still an open issue, especially when they contain reclaimed asphalt pavement (RAP) and polymer modified bitumen (PMB). In this regard, the objective of this investigation was to monitor the performance of a full-scale field trial constructed along an Italian motorway. The field trial included a section constructed with WMA mixtures (produced with a WMA chemical additive) and a reference section constructed with HMA mixtures. The WMA and HMA mixtures had the same composition (i.e., amount of RAP and PMB) and differed only for the temperatures adopted during the production of the mixtures and construction of the sections. Cored samples were taken from the binder and base courses at different times during the in-service life of the field trial (timespan of six years) and subjected to conventional testing as well as viscoelastic continuum damage (VECD) characterization. The HMA mixtures were generally stiffer than the WMA mixtures, likely due to a more marked RAP oxidation during the production and construction phases and a higher in-service ageing rate. On the contrary, the WMA mixtures always exhibited higher fatigue resistance and better homogeneity than the HMA mixtures. Based on these findings, better long-term performance is expected for the WMA section.

1. Introduction

With the increasingly stringent environmental limitations, all industries are reconsidering their production methods in order to minimize impacts. Within the framework of transportation infrastructures, the conventional hot mix asphalt (HMA) is produced and laid down at high temperatures (140–180 °C), which imply non-negligible emissions and energy consumption [1,2]. For these reasons,

* Corresponding author.
E-mail addresses: s.spadoni@pm.univpm.it (S. Spadoni), l.p.ingrassia@pm.univpm.it (L.P. Ingrassia), eumariani96@gmail.it (E. Mariani), f.cardone@univpm.it (F. Cardone), f.canestrari@univpm.it (F. Canestrari).
[1] https://orcid.org/0000-0003-0563-6473
[2] https://orcid.org/0000-0002-7184-8725
[3] https://orcid.org/0000-0002-5361-9654
[4] https://orcid.org/0000-0003-0773-6574

https://doi.org/10.1016/j.cscm.2022.e01451
Received 30 June 2022; Received in revised form 20 August 2022; Accepted 1 September 2022
Available online 2 September 2022

in the last decade, warm mix asphalt (WMA) technology has undergone a strong development [3]. WMA are mixtures produced and compacted at lower temperature (i.e., 100–140 °C) [2], through three main methodologies: foaming processes, organic additives and chemical additives [1,2,4,5]. It has been demonstrated that the use of chemical additives, which are usually a combination of surfactants, polymers, emulsification agents and aggregate coating promotors, guarantees better performance in terms of workability and moisture susceptibility, ensuring also less binder ageing [2,4,6–9]. The reduction of temperature has many beneficial effects, such as reduced emissions and energy savings (environmental and economic benefits), increased haul distance and extended paving season (technical benefits), improved working conditions (benefits for the human health) [10–14].

However, it is well-known that low temperature production results in less oxidative hardening of the binder, which could lead to a greater rutting potential [4,5]. Since in Europe styrene-butadiene-styrene (SBS) polymer modified bitumen (PMB) is widely used to increase the rutting and fatigue resistance of asphalt mixtures [15–17], some researchers investigated the effect of chemical additives on SBS modified WMA mixtures. Many studies showed the effectiveness and compatibility between these materials, which overall provide improved performance for WMA mixtures, despite the fact that SBS bitumen usually requires high production and compaction temperatures to gain proper workability [18–20]. Chemical additives have no noticeable influence on the rheological properties of SBS bitumen and Fourier transform infrared spectroscopy analysis showed broadly unaltered chemical composition for the binders [21]. Moreover, in the case of chemical additives, the workability is ensured by better interactions between bitumen and aggregates rather than by lower bitumen viscosity [6,18]. The rutting resistance and the elastic response at high temperature are enhanced due to a reduced temperature susceptibility [21,22]. In addition, the chemical additives positively affect the short-term ageing, resulting in a potential increase in fatigue resistance of the pavement [23]. The good pavement performance is demonstrated also by in-situ investigations [24,25]. However, there are limited data on the long-term performance, which remains still an open issue, especially in the case of warm recycled mixtures produced with SBS polymer modified bitumen.

Another advantage of the production at lower temperature is the possibility to incorporate high percentages of reclaimed asphalt pavement (RAP). This could lead to environmental and technical benefits, such as the reduced demand for non-renewable resources, virgin aggregates and production energy, and improved rutting performance [2,4,26,27]. One of the major challenges is to produce 100% RAP asphalt mixtures, which can be obtained only by using WMA additives and rejuvenators, capable to adjust the properties of the aged RAP binder [27]. Moreover, the workability issues of mixtures containing RAP are counterbalanced by the WMA additives, which reduce the viscosity of the binder and/or the friction at the binder-aggregate interface [6], ensuring comparable or better workability with respect to mixtures with only virgin aggregate [26,28]. However, the long-term effectiveness of these products and their interaction with the asphalt binder during in-service life are very uncertain, and, as a consequence, road agencies allow relatively low percentages of RAP in the mixtures. In addition, due to the intrinsic heterogeneity of RAP [29], researchers did not find consensus on fatigue response [26]. In fact, the fatigue resistance of recycled WMA depends on several factors, such as the type of WMA technology, the mixing method, the performance grade of the binder, the type and amount of additive/rejuvenator, as well as the source and amount of RAP [28,30]. The combination and the equilibrium between these variables must be studied case by case in order to make specific recommendations [31]. No firm conclusion was obtained about the use of organic additives [32,33], foaming process [34] and chemical additives [30,34]. For example, in [30] recycled WMA produced with chemical additive showed a lower fatigue resistance than the same WMA mixture produced with rejuvenator. In [34], the fatigue resistance of WMA produced with chemical additive was higher at short-term but had a faster decrease with ageing as compared to the control HMA mixture. In addition, it should be underlined that in all the abovementioned studies [30,32–34], a neat bitumen was employed, whereas the fatigue resistance evaluation of WMA with modified bitumen is very limited, to date.

In order to assess the fatigue performance of asphalt mixtures, the viscoelastic continuum damage (VECD) theory can be adopted successfully. Differently from most fatigue laws, the VECD model is based on the so-called damage characteristic curve and an energy-based failure criterion, which are both independent of temperature, applied stress/strain, loading frequency and mode of loading [35,36]. In literature, there are few studies on WMA containing RAP based on the VECD model, and all experiments were carried out only on laboratory specimens [37–39]. In [38], WMAs produced with 35% of RAP using an organic additive, a chemical additive and foaming technique showed lower stiffness and ageing than the reference HMA but the fatigue resistance was penalized, except for the mixture with the chemical additive. According to [37] and [39], a longer fatigue life was proved for WMA with 40÷50% RAP using rejuvenators or through the foaming process. None of these studies considered a SBS polymer modified bitumen.

Given this background, this paper presents the evolution over six years of the stiffness and fatigue properties of a WMA recycled pavement in comparison with a hot recycled pavement, both produced with SBS polymer modified bitumen and constructed along an Italian motorway. This study can improve the current knowledge of WMA scenario, towards a more conscious use of WMA produced with chemical additives and containing SBS modified bitumen and RAP. Moreover, the experimental outcomes provide valuable data on the long-term performance of a pavement constructed with such materials and subjected to actual motorway heavy traffic. The laboratory investigation of cored samples included indirect tensile tests and the VECD characterization, which has never been applied to cored samples of WMA including PMB and RAP to date.

Table 1
Aggregate gradation of the investigated mixtures.

Sieve (mm)		31.5	20	16	10	6.3	2	0.5	0.25	0.063
Passing (%)	Binder course	100	97.3	90.4	68.8	45.8	29.4	14.8	12.1	6.7
	Base course	100	96.9	91.7	68.2	44.8	28.0	13.5	11.4	6.4

2. Materials and field trial description

Four dense-graded asphalt mixtures were investigated in this study, namely a HMA and a WMA for binder courses, and a HMA and a WMA for base courses. Table 1 reports the aggregate gradation of the investigated mixtures as determined by bitumen extraction [40]. The nominal maximum aggregate size (NMAS) was equal to 16 mm.

Binder course mixtures contained 25% by aggregate weight of unfractioned 0/14 mm RAP and 4.8% by aggregate weight (4.5% by mixture weight) of total bitumen content (virgin bitumen plus bitumen from RAP). Base course mixtures contained 30% of the same unfractioned 0/14 mm RAP and 4.2% by aggregate weight (4.0% by mixture weight) of total bitumen content. For all the mixtures, the virgin and RAP bitumen were SBS polymer modified with 3.8% polymer content by bitumen weight. The amount of bitumen contained in the RAP, evaluated by bitumen extraction [40], was equal to 5.0% by aggregate weight. Table 2 reports the properties of the virgin SBS polymer modified bitumen before and after short-term ageing simulated with the Rolling Thin Film Oven Test (RTFOT).

The WMA mixtures were produced with a chemical additive (C1) mainly composed of ammine substances which act as adhesion enhancers and surfactants due to their polarized extremities [12,46]. The chemical additive C1 is characterized by a pour point of about − 8 °C and a flash point higher than 140 °C. At 25 °C, it is a viscous liquid with a density of about 1.0 g/cm^3. The dosage of C1 was equal to 0.50% and 0.55% by virgin bitumen weight for the binder course and the base course, respectively. These dosages were designed in accordance with the recommendations of producer and based on the actual "working" bitumen content (i.e., the sum of virgin bitumen and re-activated RAP bitumen), in order to consider the different amount of RAP in the binder and base courses [46,47].

The production and compaction temperatures were 130 °C and 120 °C for the WMA mixtures, and 170 °C and 160 °C for the HMA mixtures.

These materials were used to construct a full-scale field trial in April 2016 along the A1 motorway (South carriageway) in central Italy. All the details about the production of these mixtures and the construction of the field trial can be found in [12]. The construction activities consisted in the milling and re-construction of the asphalt courses of the slow lane. The field trial includes two consecutive 200-m sections, one constructed with the HMA mixtures and the other one with the WMA mixtures. The pavement structure is as follows:

- Wearing course, made of an open-graded mixture, with nominal thickness of 4 cm (not investigated in this study due to its limited thickness);
- Binder course with nominal thickness of 10 cm;
- Base course with nominal thickness of 15 cm;
- Cold recycled subbase course with nominal thickness of 25 cm.

Traffic analyses indicate that the full-scale field trial is subjected to 8.5 million equivalent single axle loads (ESALs) per year (calculated considering a 120 kN reference axle with twin wheels).

3. Testing program and methods

3.1. Testing program

Fig. 1 shows the history of testing program carried out on the field trial. Cored samples of the asphalt courses were extracted from the field trial in April 2016 (after one week from the construction and before the re-opening to traffic), in November 2019 and in January 2022 at different positions in the middle of the lane. In 2016 and 2019, 100 mm diameter cores were extracted from each section. Then, each core was cut to obtain two 50 mm height specimens from the binder and base courses, respectively. Indirect tensile stiffness modulus (ITSM) tests and indirect tensile fatigue tests (ITFT) were carried out on specimens from the binder course in 2016 and on specimens from both the binder and base courses in 2019. In 2022, 200 mm diameter cores were extracted from each section, afterwards "small" specimens (diameter of 38 mm and height of 110 mm) were horizontally cored from both the binder and base courses [48]. VECD characterization was carried out on the latter specimens cored in 2022, performing dynamic modulus tests in compression load configuration and cyclic fatigue tests in direct tension configuration on different series of small specimens.

Table 2
Properties of the virgin SBS polymer modified bitumen.

	Measured value	Reference Standard
Needle penetration at 25 °C	54 dmm	EN 1426[41]
Softening point (R&B method)	71 °C	EN 1427[42]
Elastic recovery at 25 °C; 25 cm/min	89%	EN 13398[43]
Viscosity at 135 °C	1.24 Pa·s	ASTM D4402[44]
Change in mass after RTFOT	0.05%	EN 12607–1[45]
Needle penetration at 25 °C after RTFOT	27 dmm	EN 1426[41]
Softening point (R&B method) after RTFOT	77 °C	EN 1427[42]

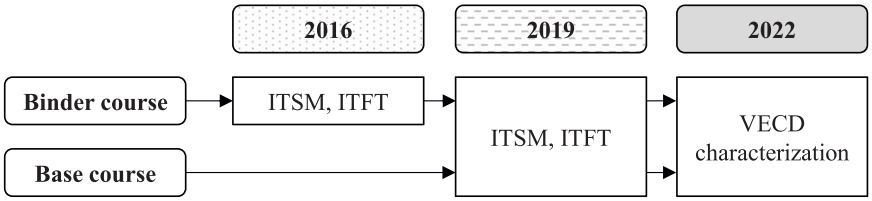

Fig. 1. History of the testing program on cored samples taken from the field trial.

3.2. Indirect tensile testing

The ITSM tests (EN 12697–26 Annex C [49]) were carried out at 20 °C by means of a servo-pneumatic machine. A repeated pulse load, with rise-time of 124 ms and pulse repetition period of 3 s (corresponding to a frequency of 2 Hz), was applied to achieve a target horizontal deformation of 5 μm. The ITSM (Eq. (1)) was calculated as the average ITSM value on two perpendicular diameters of the specimen.

$$ITSM = \frac{F_{max}(\nu + 0.273)}{t \cdot d_{max}} \tag{1}$$

where F_{max} is the peak load value, ν is the Poisson's ratio (assumed equal to 0.35), t is the average specimen thickness, and d_{max} is the amplitude of the horizontal deformation. Ten replicates were performed for each mixture.

Some of the specimens subjected to ITSM tests were then subjected to ITFT (EN 12697–24 Annex E [50]). The tests were carried out at 20 °C by means of the same servo-pneumatic machine, that applied a repeated haversine load with 0.1 s loading time and 0.4 s rest time. Initial horizontal strains between 100 and 200 με allowed to obtain a fatigue life between 10^3 and 10^6 cycles. The physical failure of the specimen was selected as failure criterion. The initial horizontal strain $\varepsilon_{h,0}$ was related to the number of cycles at failure N_f by a linear regression, derived from the Wohler's model, in a bi-logarithmic plane (Eq. (2)).

$$\log N_f = a - b \cdot \log \varepsilon_{h,0} \tag{2}$$

where a and b are material parameters, and $\varepsilon_{h,0}$ was measured at the 100th load cycle. For comparison purposes, the strain corresponding to 10^6 loading cycles (ε_6) was also calculated [50]. Six replicates were performed for each mixture.

3.3. VECD characterization

The VECD characterization included dynamic modulus tests in compression mode and cyclic fatigue tests in direct tension configuration, both carried out on small specimens by means of the Asphalt Mixture Performance Tester (AMPT).

The norm of the dynamic modulus |E *|and the phase angle θ were determined at 4 °C, 20 °C and 40 °C, as prescribed by the reference standard (AASHTO TP 132 [51]). The selected frequencies for each temperature were 0.1 Hz, 0.5 Hz, 1 Hz, 5 Hz, 10 Hz and 20 Hz. The amplitude of the sinusoidal axial compression load was adjusted to maintain an average strain level between 50 and 75 με. The 2S2P1D model (Eq. (3)), that expresses the linear viscoelastic behavior of a mixture through the combination of two springs, two parabolic element and one dashpot, was used to fit the experimental data of the storage modulus values, whose calculation is necessary for the analysis of the fatigue test results. A nonlinear optimization scheme was used to optimize simultaneously the storage modulus ($E_1 = |E^*| \cdot \cos\theta$) mastercurve and the time-temperature shift factors (Eq. (4)) [53].

$$E_1(i\omega\tau) = E_{1,0} + \frac{E_{1,\infty} - E_{1,0}}{1 + \delta(i\omega\tau)^{-k} + (i\omega\tau)^{-h} + (i\omega\beta\tau)^{-1}} \tag{3}$$

where $E_{1,\infty}$ and $E_{1,0}$ are the storage modulus values for frequency $\omega \to \infty$ and $\omega \to 0$, respectively, representing the springs (2S); k and h are parameters related to the parabolic elements (2P); δ is a proportional constant between the parabolic elements; β is correlated with the Newtonian viscosity of the dashpot (1D) [52].

$$log(a_T) = a_1 \cdot T^2 + a_2 \cdot T + a_3 \tag{4}$$

where a_1, a_2 and a_3 are fitting coefficients, and T is the testing temperature (4 °C, 20 °C and 40 °C). Three replicates were performed for each mixture.

Uniaxial cyclic fatigue tests on small specimens were carried out in control actuator displacement mode of loading at the frequency of 10 Hz (AASHTO TP 133 [53]). Before running the fatigue test, a dynamic modulus fingerprint test allowed to assess the specimen-to-specimen variability and to calibrate the strain level for the fatigue test. The testing temperature is based on the properties of the binder, and it is calculated as the average of the binder PG temperatures minus 3 °C, that must not exceed 21 °C [53]. Since the expected PG of the binder in the recycled mixtures was PG 76–16, the testing temperature was 21 °C. The test data were analyzed applying the simplified-viscoelastic continuum damage (S-VECD) theory [54]. The relationship between the integrity of the material (pseudo stiffness, C) and the amount of damage S (which is known as damage characteristic curve) is expressed by a power function

law (Eq. (5)) and describes an intrinsic property of the material independent of the test conditions [35].

$$C = 1 - C_{11} \cdot S^{C_{12}} \tag{5}$$

where C_{11} and C_{12} are the fitting coefficients. At least three replicates with overlapping C vs. S curves were considered for each mixture.

D^R (Eq. (6)) is the parameter representing the failure criterion [36]. It is the average reduction in pseudo stiffness up to failure and is a measure of the material toughness. The number of cycles to failure N_f is defined as the cycle in which the product given by peak-to-peak stress and cycle number reaches a maximum value after a stable increase during cyclic loading [53].

$$D^R = \frac{\int_0^{N_f} (1 - C) dN}{N_f} = \frac{Cum(1 - C)}{N_f} \tag{6}$$

The stiffness, damage characteristics and toughness are taken into account by the synthetic index S_{app} (Eq. (7)), which expresses the fatigue resistance of the asphalt mixture [53]. S_{app} refers to a temperature which is determined as the average climatic PG temperature of the pavement location, minus 3 °C [53]. Since the field trial is in a PG 58–10 climatic zone [55], S_{app} reference temperature was equal to 21 °C.

$$S_{app} = 1000^{\left(\frac{\alpha}{2}-1\right)} \cdot \frac{a_{T(S_{app})}^{\frac{1}{\alpha+1}} \cdot \left(\frac{D^R}{C_{11}}\right)^{\frac{1}{C_{12}}}}{|E^*|^{\frac{\alpha}{4}}_{LVE,Sapp}} \tag{7}$$

where α is the damage growth rate; $\alpha_{T(Sapp)}$ is the time-temperature shift factor between the S_{app} temperature and the reference temperature considered for the dynamic modulus mastercurve; and $|E^*|^{\frac{\alpha}{4}}_{LVE,Sapp}$ is the reference modulus calculated at the S_{app} reference temperature and at the reduced frequency of $62.8 \cdot \alpha_{T(Sapp)}$. S_{app} values are usually between 0 and 50, specifically higher values indicate better fatigue resistance [56,57].

4. Results and analysis

4.1. Binder course mixtures

4.1.1. Indirect tensile properties

Fig. 2 presents the evolution of the stiffness modulus values during the six years of the pavement in-service life for both mixture types (HMA and WMA). The average air void content (A.V.) of the tested specimens is also indicated. For the 2016 and 2019 data, the stiffness moduli refer to the average measured ITSM values, and the standard deviation is reported as well. For comparison purposes, for the 2022 data, the stiffness moduli refer to the dynamic modulus values calculated through the 2S2P1D model (see Section 4.1.2) at the same testing conditions as for the ITSM tests (temperature of 20 °C, frequency of 2 Hz). Since these values come from a model fitted to already averaged experimental values, no standard deviation is available.

As can be observed, cores extracted in 2016 were characterized by similar volumetric properties and similar stiffness moduli. These data demonstrate that the WMA additive ensures a compactability comparable to HMA despite the reduced production and compaction temperatures (i.e., 40 °C lower), and does not negatively affect the stiffness properties [46], which are strictly related to the volumetric ones. Comparing the cores extracted in 2019 to those extracted in 2016, HMA showed significantly higher stiffness modulus in 2019, whereas WMA showed broadly unchanged results. The higher stiffness of HMA can be ascribable to a higher in-service ageing rate. The higher data dispersion of HMA in both 2016 and 2019 can be likely due to the presence of highly oxidized RAP not homogenously distributed within the mixture at the specimen scale. The high oxidation of RAP can be caused by the typical HMA production and compaction temperatures [38,46]. As for the 2022 data, it must be kept in mind that such stiffness values were

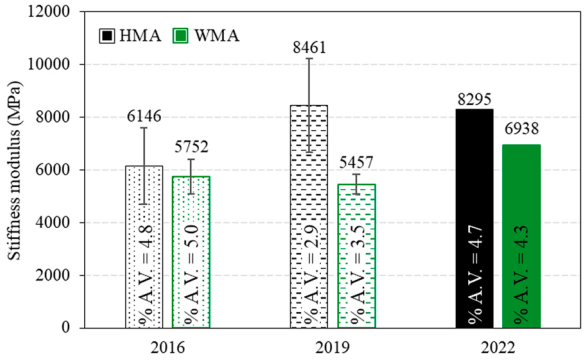

Fig. 2. Binder course mixtures: stiffness modulus values in 2016, 2019 and 2022 (error bars represent the standard deviation).

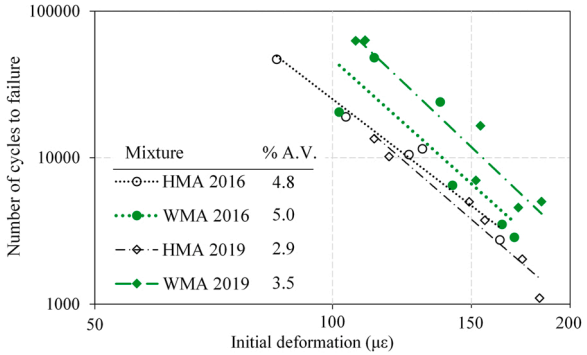

Fig. 3. Binder course mixtures: fatigue curves in 2016 and 2019.

Table 3
Binder course mixtures: fitting parameters of the fatigue curves.

		a	*b*	R^2	ε_6
2016	HMA	12.675	4.138	0.965	41
	WMA	14.344	4.836	0.724	53
2019	HMA	13.741	4.670	0.954	45
	WMA	15.203	5.115	0.927	63

measured in compression mode, which usually leads to higher stiffness values than those obtained in indirect tensile mode (2019 data). For WMA a higher stiffness was observed in 2022 as compared to 2019, whereas this was not observed for HMA. The high data variability found for HMA in 2019 can justify this finding. Moreover, the stiffness results of 2022 confirmed the trend of 2019, denoting a higher stiffness for the HMA mixture with respect to the WMA mixture, despite their comparable volumetric properties.

Fig. 3 presents the fatigue curves obtained from the specimens extracted in 2016 and 2019, whose average A.V. is indicated as well, whereas Table 3 reports the fitting parameters and the ε_6 values. In both 2016 and 2019, the linear regressions were characterized by similar slope, as demonstrated by the *b* values in Table 3 (see Eq. (2)). This outcome means that the two mixtures (HMA and WMA) had comparable sensitivity to the strain level, which did not change significantly during the first years of in-service life. However, the comparison of the curves (Fig. 3) shows the enhanced fatigue response of WMA, as also confirmed by the higher ε_6 values in both 2016 and 2019 (Table 3). This indicates a better resistance to cyclic loads for WMA, which can be ascribable to its lower stiffness with respect to HMA (Fig. 2), especially in 2019. Conversely, the higher stiffness of HMA, combined with its heterogeneity caused by the highly oxidized RAP, led to a more brittle behavior.

4.1.2. VECD properties

Fig. 4 (a) and (b) show the storage modulus and phase angle mastercurves at 21.1 °C, respectively, for the mixtures tested in 2022. Fig. 4 (a) also reports the average A.V. of the tested specimens, which had similar volumetric properties for the two mixtures. It is possible to notice that HMA exhibited higher stiffness, confirming that the higher RAP oxidation and faster in-service ageing affected its stiffness properties in a wide range of frequencies. Moreover, the higher phase angle values of WMA (Fig. 4 (b)) highlighted a more viscous and less elastic behavior with respect to HMA. Fig. 4 (c) reports the shift factors and the equations of the related linear regressions. The similar slope values (i.e., 0.132 and 0.123 for HMA and WMA, respectively) indicate that the mixtures were characterized by the same thermal susceptibility, which did not depend on the different production process but can be mainly related to the bituminous components (virgin bitumen and bitumen from RAP), which are the same for both mixtures. This outcome confirms that chemical additives usually do not significantly affect the rheological properties of the binder itself [4,21].

Fig. 5 (a) presents the fitting of the damage characteristic curves, obtained from three overlapping experimental curves, along with the values of fitting coefficients. The A.V. of the specimens investigated in the fatigue tests, reported in the same figure, was similar to that of the specimens investigated in dynamic modulus tests (Fig. 4 (a)). The shape of the *C* versus *S* curves for the two mixtures was comparable, indicating that the evolution of the damage in the materials was broadly the same. This outcome is consistent with the comparable sensitivity to the strain level, denoted by the similar slope of the fatigue curves in 2016 and 2019 (Fig. 3). Nevertheless, the curve of WMA was characterized by lower pseudo stiffness value *C* and higher amount of damage *S* at failure with respect to HMA, indicating a higher tolerance to damage and a postponed failure. These findings agree with the higher ε_6 values for WMA extrapolated from the fatigue curves in 2016 and 2019 (Table 3). Fig. 5 (b) presents the D^R failure envelopes. The D^R values are the slopes of the linear relationships reported in the figure. WMA showed a slightly higher D^R value (0.736), which indicates a higher toughness, i.e., better ability to absorb energy before failure. Fig. 5 (c) shows the S_{app} values, together with the average A.V. of all tested specimens (dynamic modulus and cyclic fatigue tests). The S_{app} ranking reflects the previous observations on the *C* versus *S* curves and D^R values, highlighting that a better fatigue performance can be expected from WMA.

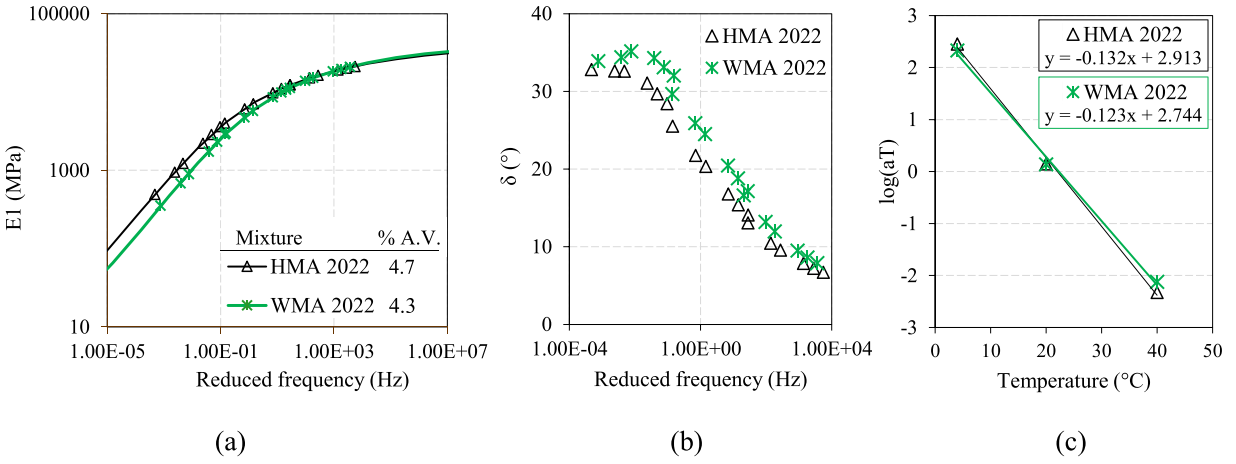

Fig. 4. Binder course mixtures: **(a)** storage modulus mastercurves (2S2P1D model) and **(b)** phase angle mastercurves at 21.1 °C, **(c)** shift factors.

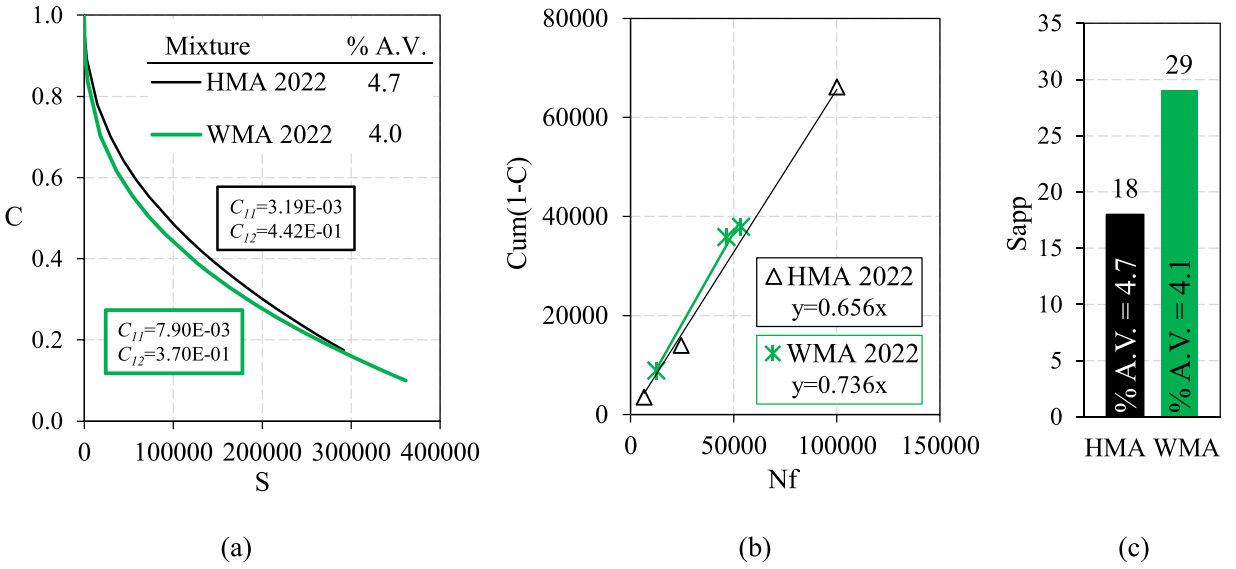

Fig. 5. Binder course mixtures: **(a)** fitting of the damage characteristic curves, **(b)** D^R failure criterion and **(c)** S_{app} values.

4.2. Base course mixtures

4.2.1. Indirect tensile properties

Fig. 6 presents the stiffness modulus values obtained from the specimens cored in 2019 and 2022 for both types of mixture (HMA and WMA). The average A.V. is indicated in the figure as well. The average ITSM values and the related standard deviations are reported for the 2019 specimens, whereas the dynamic modulus values derived from the 2S2P1D model at the same testing conditions as for the ITSM tests are reported for the 2022 specimens (as already explained in Section 4.1.1). First, it is worth pointing out that WMA reached an average A.V. about 1% lower than HMA. This can be likely due to the chemical additive used for the WMA production, which ensured a proper compactability of the mixture. In 2019, cored samples of both mixtures showed similar stiffness despite the different volumetric properties. This can be attributed to the stronger RAP oxidation during the production and construction phases and the faster in-service ageing rate undergone by the HMA mixture as compared to the WMA mixture. As for the comparison between 2019 and 2022 results, recall that the stiffness moduli were obtained in compression mode in 2022 versus indirect tensile mode in 2019. As already mentioned in Section 4.1.1, the compression mode should imply higher stiffness values. A higher stiffness was observed for WMA in 2022 as compared to 2019, whereas HMA showed a stiffness decrease of about 18% in the same period. This decrease can be ascribable to a certain extent to the different A.V. observed for HMA in 2019 and 2022, even though the inhomogeneity of the HMA mixture is considered as the main cause. As anticipated in Section 3.1, the samples were obviously cored in different positions of the trial section. In this regard, the properties of the HMA section seem to change more from point to point, as denoted by

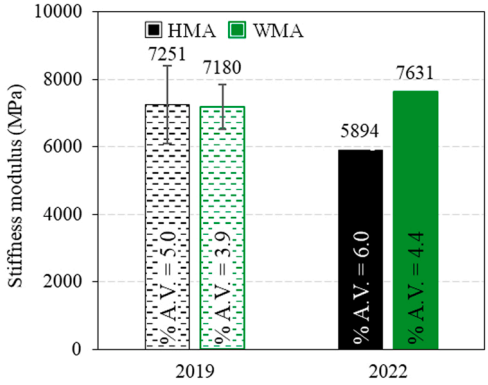

Fig. 6. Base course mixtures: stiffness modulus values in 2019 and 2022 (error bars represent the standard deviation).

the higher standard deviation (Fig. 6), although the production and construction phases were strictly controlled. These results support that WMA is a more homogenous material with comparable performance along the pavement.

Fig. 7 presents the fatigue curves obtained from the specimens cored in 2019, whose average A.V. is also indicated, whereas Table 4 reports the fitting parameters and the ε_6 values. The linear regression of HMA was characterized by a lower slope, which means a lower sensitivity to the applied deformation level. On the other hand, WMA exhibited a significantly higher ε_6 value (i.e., 60 με vs. 28 με), which suggests a longer fatigue life for small deformations (such as those to which a thick pavement is typically subjected). Moreover, in 2019, WMAs of binder and base courses were characterized by similar A.V. (Fig. 3, Fig. 7) and similar fatigue behavior, as expressed by a and b values of Eq. (2) and ε_6 value (Table 3, Table 4). In this regard, the chemical additive allowed to reach similar properties for the binder and base courses, even though the base mixture was characterized by higher RAP content and lower virgin bitumen content with respect to the binder mixture (in the light of a comparable aggregate gradation, see Section 2). On the contrary, for the HMAs, the volumetric properties and mechanical behavior of the binder and base courses were different. In this case, the compactability of the base course was penalized by the higher RAP content and the lower virgin bitumen content as well as the greater layer thickness with respect to the binder course.

4.2.2. VECD properties

Fig. 8 (a) presents the storage modulus mastercurves at 21.1 °C and the average A.V. of the specimens tested in 2022. WMA showed higher stiffness with respect to HMA, mainly due to the lower A.V. of the WMA mixture. Fig. 8 (b) presents the phase angle mastercurves at 21.1 °C. It can be observed that the phase angle values are broadly the same for the two mixtures. Fig. 8 (c) reports the shift factors and the equations of the related linear regressions. The shift factor values and regression curves basically overlapped and were also similar to those obtained for the binder course (Fig. 4 (c)). This confirms that the thermal susceptibility is mainly affected by the bitumen properties, which do not change even in the presence of the additive.

Fig. 9 (a) presents the fit of the damage characteristic curves, obtained from at least three overlapping experimental curves, along with the average A.V. of the specimens tested and the values of the fitting coefficients. First, it should be noted that the different in-situ A.V. of the mixtures (i.e., about 2.5% difference) significantly influenced their fatigue behavior, as discussed in detail below. The higher position of the WMA curve was consistent with the stiffness properties and A.V., confirming that the curve of softer mixtures tends to stay below that of stiffer mixtures [58].

Both curves showed similar pseudo stiffness C at failure, indicating a comparable tolerance to damage, whereas WMA curve reached higher S value at failure, indicating a lower rate of fatigue resistance loss during the in-service life. This outcome reflects the higher ε_6 value observed for WMA from the 2019 fatigue curves (Table 4), suggesting a longer fatigue life for WMA. Fig. 9 (b) presents the failure envelopes, whose slope corresponds to D^R. A higher D^R value was observed for the HMA mixture, denoting its greater ability to absorb energy before failure, which is strictly related to its lower stiffness (Fig. 8 (a)) mostly due to the higher A.V. Fig. 9 (c) shows the S_{app} values and the average A.V. of all tested specimens (dynamic modulus and cyclic fatigue tests). In this case, the S_{app} ranking did not confirm the D^R ranking, because the S_{app} value depends also on the stiffness properties and the damage characteristics (Eq. (7)). The higher S_{app} value obtained for WMA can be explained by considering that the WMA mixture has better damage properties (Fig. 9 (a)) and its higher stiffness (Fig. 8 (a)), linked to the A.V., ensures a better distribution of the strains/stresses within the pavement. Analogously to the binder course, a better fatigue performance can be thus expected from WMA even for the base course. In addition, analogously to what observed for the fatigue curves of WMAs obtained in 2019, the damage characteristic curves of WMAs obtained in 2022 for binder and base courses were characterized by a similar shape (as denoted by comparable C_{11} and C_{12} values) and similar C and S values at failure (around 0.1 and 380000, respectively) (Fig. 5, Fig. 9). This finding corroborates the beneficial effect of the WMA additive on the volumetric properties of the mixture, despite the higher RAP content and the lower bitumen content of the base course with respect to the binder course.

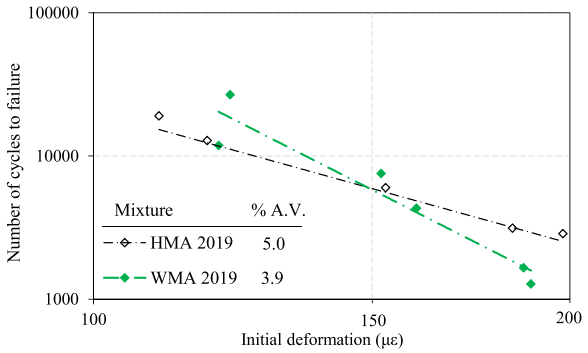

Fig. 7. Base course mixtures: fatigue curves in 2019.

Table 4
Base course mixtures: fitting parameters of the fatigue curves.

		a	*b*	R^2	ε_6
2019	HMA	10.435	3.062	0.905	28
	WMA	15.995	5.621	0.913	60

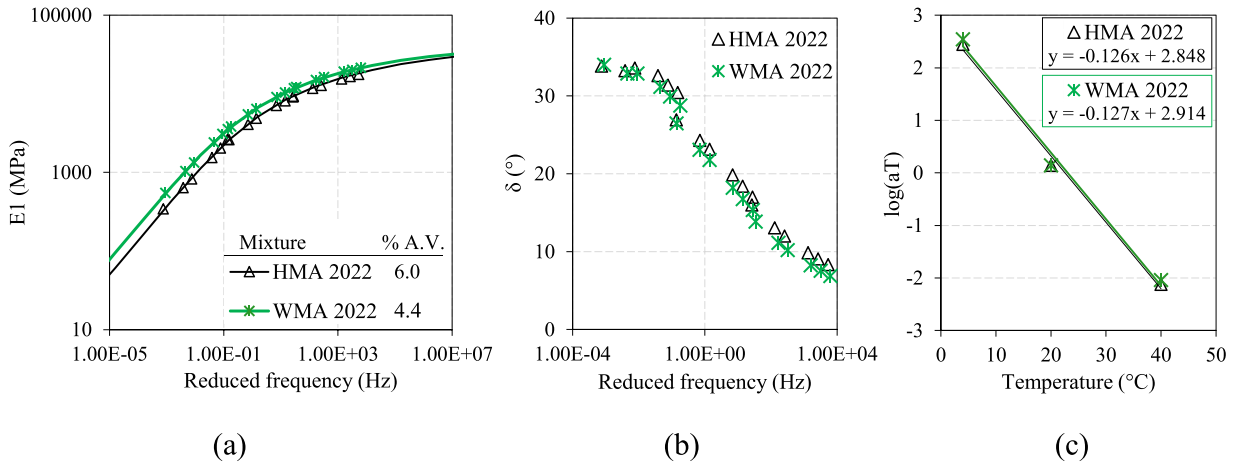

Fig. 8. Base course mixtures: **(a)** storage modulus mastercurves (2S2P1D model) and **(b)** phase angle mastercurves at 21.1 °C, **(c)** shift factors.

5. Conclusions

The objective of this investigation was to monitor the performance of a full-scale field trial constructed along an Italian motorway, which included a section constructed with WMA mixtures (produced with a WMA chemical additive) and a reference section constructed with conventional HMA mixtures. The WMA and HMA mixtures had the same composition (i.e., amount of RAP and PMB) and differed only for the adopted production and compaction temperatures (40 °C lower for WMA). The characterization was carried out by means of laboratory testing performed on cored samples taken from the binder and base courses of the field trial pavement. In 2016 (year of construction) and 2019, conventional indirect tensile tests were carried out, whereas in 2022 the VECD characterization was considered.

Immediately after the construction (2016), WMA showed comparable stiffness properties and improved fatigue resistance with respect to HMA. However, during the in-service life, the stiffness of HMA increased much more than WMA stiffness and it was characterized by a high dispersion of the results. These findings are likely due to a stronger RAP oxidation during the production and construction phases (caused by the high temperatures adopted for HMA) and a higher in-service ageing rate experienced by the HMA section. These factors negatively affected the fatigue performance, leading to a more brittle behavior and a reduced toughness, as demonstrated by lower ε_6 (2019) and S_{app} values (2022).

On the contrary, WMA showed more homogenous properties along the trial section in both binder and base courses. Regarding the fatigue properties, WMA was characterized by a greater tolerance to damage and a slower rate of fatigue resistance loss during the in-service life as compared to HMA. Moreover, for both binder and base courses, the similar shift factor values obtained for HMA and

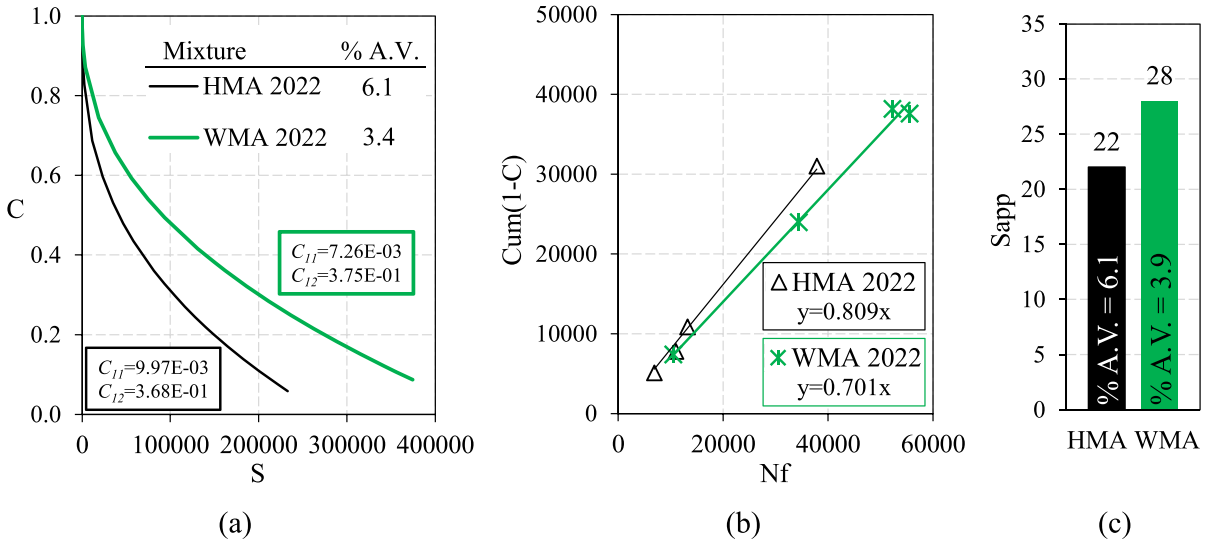

Fig. 9. Base course mixtures: **(a)** fitting of the damage characteristic curves, **(b)** D^R failure criterion and **(c)** S_{app} values.

WMA showed that the chemical additive did not alter the thermal susceptibility of the mixture, confirming that the latter depends strictly on the bituminous components (virgin bitumen and bitumen from RAP).

Moreover, it is worth pointing out that the VECD results confirmed the trend of the conventional indirect tensile tests, giving at the same time additional information about the intrinsic properties of the materials and demonstrating the reliability of the VECD model even for WMA mixtures. Further advantages of the VECD characterization are less time-consuming laboratory tests and less cores to be extracted from the pavement, thanks to the small specimen geometry.

These findings, gathered during a relatively wide timespan of pavement in-service life, suggest that the WMA section has better long-term performance with respect to the reference HMA section, demonstrating the compatibility between the PMB and the chemical additive throughout in-service ageing as well. Considering also the significant environmental and economic benefits ensured by WMA technologies, warm recycled mixtures produced with WMA chemical additives and PMB represent a reliable and environmentally friendly solution to obtain durable pavements. The existing field trial will be continuously monitored over time, providing further data regarding the evolution of the behavior of these mixtures in the field.

Funding

This research did not receive any specific grant from funding agencies in the public, commercial, or not-for-profit sectors.

Declaration of Competing Interest

The authors declare that they have no known competing financial interests or personal relationships that could have appeared to influence the work reported in this paper.

Data Availability

Data will be made available on request.

Acknowledgements

The activities presented in this paper were sponsored by Pavimental S.p.A. (Italy), which gave both financial and technical support within the framework of the Extreme Recycling of Asphalt (ERA) project. The results and opinions presented are those of the authors.

References

[1] M.C. Rubio, G. Martínez, L. Baena, F. Moreno, Warm mix asphalt: an overview, J. Clean. Prod. 24 (2012) 76–84, https://doi.org/10.1016/j.jclepro.2011.11.053.
[2] G. Cheraghian, A. Cannone Falchetto, Z. You, S. Chen, Y.S. Kim, J. Westerhoff, K.H. Moon, M.P. Wistuba, Warm mix asphalt technology: an up to date review, J. Clean. Prod. 268 (2020), 122128, https://doi.org/10.1016/j.jclepro.2020.122128.
[3] A. Abed, N. Thom, J. Grenfell, A novel approach for rational determination of warm mix asphalt production temperatures, Constr. Build. Mater. 200 (2019) 80–93, https://doi.org/10.1016/j.conbuildmat.2018.12.082.

[4] A. Behnood, A review of the warm mix asphalt (WMA) technologies: Effects on thermo-mechanical and rheological properties, J. Clean. Prod. 259 (2020), 120817, https://doi.org/10.1016/j.jclepro.2020.120817.
[5] S.D. Capitão, L.G. Picado-Santos, F. Martinho, Pavement engineering materials: Review on the use of warm-mix asphalt, Constr. Build. Mater. 36 (2012) 1016–1024, https://doi.org/10.1016/j.conbuildmat.2012.06.038.
[6] L.P. Ingrassia, X. Lu, F. Canestrari, G. Ferrotti, Tribological characterization of bituminous binders with Warm Mix Asphalt additives, Constr. Build. Mater. 172 (2018) 309–318, https://doi.org/10.1016/j.conbuildmat.2018.03.275.
[7] R. Pereira, A. Almeida-Costa, C. Duarte, A. Benta, Warm mix asphalt: Chemical additives' effects on bitumen properties and limestone aggregates mixture compactibility, Int. J. Pavement Res. Technol. 11 (3) (2018) 285–299, https://doi.org/10.1016/j.ijprt.2017.10.005.
[8] A. Kusam, H. Malladi, A.A. Tayebali, N.P. Khosla, Laboratory evaluation of workability and moisture susceptibility of warm-mix asphalt mixtures containing recycled asphalt. pavements, J. Mater. Civ. Eng. 29 (5) (2017), 04016276, https://doi.org/10.1061/(ASCE)MT.1943-5533.0001825.
[9] X. Liang, X. Yu, C. Chen, G. Ding, J. Huang, Towards the low-energy usage of high viscosity asphalt in porous asphalt pavements: a case study of warm-mix asphalt additives, Case Stud. Constr. Mater. 16 (2022), e00914, https://doi.org/10.1016/j.cscm.2022.e00914.
[10] A. Almeida-Costa, A. Benta, Economic and environmental impact study of warm mix asphalt compared to hot mix asphalt, J. Clean. Prod. 112 (2016) 2308–2317, https://doi.org/10.1016/j.jclepro.2015.10.077.
[11] A. Vaitkus, D. Čygas, A. Laurinavičius, V. Vorobjovas, Z. Perveneckas, Influence of warm mix asphalt technology on asphalt physical and mechanical properties, Constr. Build. Mater. 112 (2016) 800–806, https://doi.org/10.1016/j.conbuildmat.2016.02.212.
[12] Stimilli A., Frigio F., Canestrari F., Sciolette S. (2017, April 10–12). In-plant production of warm recycled mixtures produced with SBS modified bitumen: A case study, Transport Infrastructure and systems. Proceedings of the AIIT International Congress on Transport Infrastructure and Systems, TIS 2017, Rome, Italy (pp. 143–151).
[13] A. Almusawi, B. Sengoz, D.K. Ozdemir, A. Topal, Economic and environmental impacts of utilizing lower production temperatures for different bitumen samples in a batch plant, Case Stud. Constr. Mater. 16 (2022), e00987, https://doi.org/10.1016/j.cscm.2022.e00987.
[14] X. Yang, Z. You, D. Perram, D. Hand, Z. Ahmed, W. Wei, S. Luo, Emission analysis of recycled tire rubber modified asphalt in hot and warm mix conditions, J. Hazard. Mater. 365 (2019) 942–951, https://doi.org/10.1016/j.jhazmat.2018.11.080.
[15] G.D. Airey, Styrene butadiene styrene polymer modification of road bitumens, J. Mater. Sci. 39 (3) (2004) 951–959, https://doi.org/10.1023/B:JMSC.0000012927.00747.83.
[16] P. Lin, C. Yan, W. Huang, Y. Li, L. Zhou, N. Tang, F. Xiao, Y. Zhang, Q. Lv, Rheological, chemical and aging characteristics of high content polymer-modified asphalt, Constr. Build. Mater. 207 (2019) 616–629, https://doi.org/10.1016/j.conbuildmat.2019.02.086.
[17] A. Behnood, M. Modiri Gharehveran, Morphology, rheology, and physical properties of polymer-modified asphalt binders, Eur. Polym. J. 112 (2019) 766–791, https://doi.org/10.1016/j.eurpolymj.2018.10.049.
[18] A. Stimilli, A. Virgili, F. Canestrari, Warm recycling of flexible pavements: effectiveness of warm mix asphalt additives on modified bitumen and mixture performance, J. Clean. Prod. 156 (2017) 911–922, https://doi.org/10.1016/j.jclepro.2017.03.2351.
[19] A.V. Kataware, D. Singh, Effect of short-term ageing on high-temperature performance of SBS modified binder containing warm mix asphalt additives, Road. Mater. Pavement Des. 21 (3) (2020) 623–642, https://doi.org/10.1080/14680629.2018.1509804.
[20] S. Zhang, D. Wang, F. Guo, et al., Properties investigation of the SBS modified asphalt with a compound warm mix asphalt (WMA) fashion using the chemical additive and foaming procedure, J. Clean. Prod. 319 (2021), 128789, https://doi.org/10.1016/j.jclepro.2021.128789.
[21] G. Ferrotti, D. Ragni, X. Lu, F. Canestrari, Effect of warm mix asphalt chemical additives on the mechanical performance of asphalt binders, Mater. Struct. 50 (2017) 226, https://doi.org/10.1617/s11527-017-1096-5.
[22] F. Morea, R. Marcozzi, G. Castaño, Rheological properties of asphalt binders with chemical tensoactive additives used in Warm Mix Asphalts (WMAs), Constr. Build. Mater. 29 (2012) 135–141, https://doi.org/10.1016/j.conbuildmat.2011.10.010.
[23] D. Ragni, G. Ferrotti, X. Lu, F. Canestrari, Effect of temperature and chemical additives on the short-term ageing of polymer modified bitumen for WMA, Mater. Des. 160 (2018) 514–526, https://doi.org/10.1016/j.matdes.2018.09.042.
[24] F. Frigio, A. Stimilli, A. Virgili, F. Canestrari, Performance assessment of in plant produced warm recycled mixtures for open-graded wearing courses, Transp. Res. Rec. (2017), https://doi.org/10.3141/2633-04.
[25] Stimilli A., Frigio F., Cardone F., Canestrari F. Performance of warm recycled mixtures in field trial sections. Proceedings of BCRRA 2017, June 28–30, Athens, Greece.
[26] M. Guo, H. Liu, Y. Jiao, L. Mo, Y. Tan, D. Wang, M. Liang, Effect of WMA-RAP technology on pavement performance of asphalt mixture: a state-of-the-art review, J. Clean. Prod. 266 (2020), 121704, https://doi.org/10.1016/j.jclepro.2020.121704.
[27] M. Rathore, V. Haritonovs, R. Merijs Meri, M. Zaumanis, Rheological and chemical evaluation of aging in 100% reclaimed asphalt mixtures containing rejuvenators, Constr. Build. Mater. 318 (2022), 126026, https://doi.org/10.1016/j.conbuildmat.2021.126026.
[28] F. Xiao, N. Su, S. Yao, S. Amirkhanian, J. Wang, Performance grades, environmental and economic investigations of reclaimed asphalt pavement materials, J. Clean. Prod. 211 (2019) 1299–1312, https://doi.org/10.1016/j.jclepro.2018.11.126.
[29] V. Antunes, A.C. Freire, J. Neves, A review on the effect of RAP recycling on bituminous mixtures properties and the viability of multi-recycling, Constr. Build. Mater. 211 (2019) 453–469, https://doi.org/10.1016/j.conbuildmat.2019.03.258.
[30] D.X. Lu, M. Saleh, N.H.T. Nguyen, Effect of rejuvenator and mixing methods on behaviour of warm mix asphalt containing high RAP content, Constr. Build. Mater. 197 (2019) 792–802, https://doi.org/10.1016/j.conbuildmat.2018.11.205.
[31] C. Hettiarachchi, X. Hou, J. Wang, F. Xiao, A comprehensive review on the utilization of reclaimed asphalt material with warm mix asphalt technology, Constr. Build. Mater. 227 (2019), 117096, https://doi.org/10.1016/j.conbuildmat.2019.117096.
[32] D. Singh, Comparison of moisture and fracture damage resistance of hot and warm asphalt mixes containing reclaimed pavement materials, Constr. Build. Mater. 157 (2017) 1145–1153, https://doi.org/10.1016/j.conbuildmat.2017.09.176.
[33] D. Wang, C. Riccardi, B. Jafari, A. Cannone Falchetto, M.P. Wistuba, Investigation on the effect of high amount of Re-recycled RAP with Warm mix asphalt (WMA) technology, Constr. Build. Mater. 312 (2021), 125395, https://doi.org/10.1016/j.conbuildmat.2021.125395.
[34] M. Perez-Martinez, P. Marsac, T. Gabet, F. Hammoum, M. de Mesquita Lopes, S. Pouget, Effects of Ageing on Warm Mix Asphalts with High Rates of Reclaimed Asphalt Pavement, in: A. Chabot, W.G. Buttlar, E.V. Dave, C. Petit, G. Tebaldi (Eds.), 8th RILEM International Conference on Mechanisms of Cracking and Debonding in Pavements, RILEM Bookseries, Vol 13, Springer, Netherlands, 2016, pp. 113–118, https://doi.org/10.1007/978-94-024-0867-6_16.
[35] J.S. Daniel, Y.R. Kim, Development of a simplified fatigue test and analysis procedure using a viscoelastic damage model, J. Assoc. Asph. Paving Technol. 71 (2002) 619–650.
[36] Y.D. Wang, Y.R. Kim, Development of a pseudo strain energy-based fatigue failure criterion for asphalt mixtures, Int. J. Pavement Eng. 20 (10) (2019) 1182–1192, https://doi.org/10.1080/10298436.2017.1394100.
[37] M. Sabouri, Y.T. Choi, Y. Wang, S. Hwang, C. Baek, Y.R. Kim, Effect of Rejuvenator on Performance Properties of WMA Mixtures with High RAP Content, in: F. Canestrari, M.N. Partl (Eds.), 8th RILEM International Symposium on Testing and Characterization of Sustainable and Innovative Bituminous Materials, RILEM Bookseries, Vol 11, Springer, Netherlands, 2016, pp. 473–484, https://doi.org/10.1007/978-94-017-7342-3_38.
[38] D. Kim, A. Norouzi, S. Kass, T. Liske, Y.R. Kim, Mechanistic performance evaluation of pavement sections containing RAP and WMA additives in Manitoba, Constr. Build. Mater. 133 (2017) 39–50, https://doi.org/10.1016/j.conbuildmat.2016.12.035.
[39] F.R.G. Padula, S. Nicodemos, J.C. Mendes, R. Willis, A. Taylor, Evaluation of fatigue performance of high RAP-WMA mixtures, Int. J. Pavement Res. Technol. 12 (4) (2019) 430–434, https://doi.org/10.1007/s42947-019-0051-y.
[40] EN 12697–1: 2020. Bituminous Mixtures - Test Methods - Part 1: Soluble binder content.
[41] EN 1426: 2015. Bitumen and bituminous binders – Determination of needle penetration.
[42] EN 1427: 2015. Bitumen and bituminous binders – Determination of the softening point – Ring and Ball method.
[43] EN 13398: 2017. Bitumen and bituminous binders – Determination of the elastic recovery of modified bitumen.

[44] ASTM D4402: 2006. Standard Test Method for Viscosity Determination of Asphalt at Elevated Temperatures Using a Rotational Viscometer.
[45] EN 12607–1: 2014. Bitumen and bituminous binders – Determination of the resistance to hardening under influence of heat and air – Part 1: RTFOT method.
[46] L.P. Ingrassia, F. Cardone, G. Ferrotti, F. Canestrari, Monitoring the evolution of the structural properties of warm recycled pavements with Falling Weight Deflectometer and laboratory tests, Road. Mater. Pavement Des. 22 (sup1) (2021) S69–S82, https://doi.org/10.1080/14680629.2021.1906302.
[47] A. Stimilli, A. Virgili, F. Canestrari, New method to estimate the "re-activated" binder amount in recycled hot-mix asphalt, Road. Mater. Pavement Des. 16 (sup1) (2015) 442–459, https://doi.org/10.1080/14680629.2015.1029678.
[48] AASHTO PP 99: 2019. Standard Practice for Preparation of Small Cylindrical Performance Tests Specimens Using the Superpave Gyratory Compactor (SGC) or Field Cores.
[49] EN 12697–26: 2018. Bituminous Mixtures - Test Methods - Part 26: Stiffness.
[50] EN 12697–24:2018. Bituminous mixtures - Test methods - Part 24: Resistance to fatigue.
[51] AASHTO TP 132: 2019. Standard Method of Test for Determining the Dynamic Modulus for Asphalt Mixtures Using Small Specimens in the Asphalt Mixture Performance Tester (AMPT).
[52] F. Olard, H. Di Benedetto, General 2S2P1D model and relation between the linear viscoelastic behaviours of bituminous binders and mixes, Road. Mater. Pavement Des. 4 (2) (2003) 185–224, https://doi.org/10.1080/14680629.2003.9689946.
[53] AASHTO TP 133: 2021. Standard Method of Test for Determining the Damage Characteristic Curve and Failure Criterion Using Small Specimens in the Asphalt Mixture Performance Tester (AMPT) Cyclic Fatigue Test.
[54] B.S. Underwood, Y.R. Kim, M.N. Guddati, Improved calculation method of damage parameter in viscoelastic continuum damage model, Int. J. Pavement Eng. 11 (6) (2010) 459–476, https://doi.org/10.1080/10298430903398088.
[55] F. Giuliani, Definizione di una mappa nazionale di Performance Grade dei bitumi stradali. Quarry and Construction 527 (2006) 1–12.
[56] Y.D. Wang, B.S. Underwood, Y.R. Kim, Development of a fatigue index parameter, Sapp, for asphalt mixes using viscoelastic continuum damage theory, Int. J. Pavement Eng. 23 (2) (2022) 438–452, https://doi.org/10.1080/10298436.2020.1751844.
[57] U.S. Department of Transportation-Federal Highway Administration. Office of Preconstruction, Construction, and Pavements. Cyclic Fatigue Index Parameter (Sapp) for Asphalt Performance Engineered Mixture Design. TechBrief FHWA-HIF-19–091. 2019.
[58] T. Hou, B.S. Underwood, Y.R. Kim, Fatigue performance prediction of North Carolina mixtures using simplified viscoelastic continuum damage model, J. Assoc. Asph. Paving Technol. 79 (2010) 35–80.